Solid-state isomerization of ruthenium(II) isocyanide complexes*

Kazuko Katsuki, Yoshie Ooyama, Miki Okamoto and Yasuhiro Yamamoto**
Department of Chemistry, Faculty of Science, Toho University, Miyama 2-2-1, Funabashi, Chiba 274 (Japan)

(Received October 4, 1993; revised November 17, 1993)

Abstract

Solid-state rearrangements of *trans*-$RuCl_2(RNC)_4$ (*trans*-**1**) or *ttt*-$RuCl_2(RNC)_2(PR'_3)_2$ (*ttt*-**2**) to *cis*-$RuCl_2(RNC)_4$ (*cis*-**1**) and *tcc*-$RuCl_2(RNC)_2(PR'_3)_2$ (*tcc*-**2**) and their electrochemical reactions were examined. The enthalpy of the *trans*-**1** to *cis*-**1** isomerization is smaller than that of *ttt*-**2** to *tcc*-**2** isomerization and these isomerizations proceeded to the thermodynamically more stable isomers. Electrochemical oxidations of these complexes were quasi-reversible and the oxidation potentials of *trans* and *ttt* isomers are smaller than those of *cis* and *tcc* isomers, respectively. These results were discussed in relation to the results of EHMO calculations.

Key words: Isomerization; Ruthenium complexes; Isocyanide complexes

Introduction

Solid-state rearrangements are well known for PtL_2X_2 complexes (L = neutral donor ligand; X = halogen) [1, 2] and for cobalt(III) and chromium(III) complexes [3]. Recently, Nelson and co-workers showed that a series of *trans*-$RuCl_2(PR_3)_3(CO)$ and *ttt*-$RuCl_2(PR_3)_2(CO)_2$ complexes underwent solid-phase rearrangements [4]. Six-coordinate ruthenium(II) complexes containing isocyanides, *ttt*-$RuX_2(EtNC)_2(APh_3)_2$ (X = Cl, Br; A = P, As, Sb) isomerize in solution [5]. Complex $RuCl_2(t\text{-}BuNC)_2(PPh_3)_2$ is known to undergo photoisomerization [6].

We have investigated the solid-state rearrangements of this series of isocyanide complexes using thermal gravimetric analysis (TG) and differential scanning calorimetry (DSC), and have studied the electrochemistry of these complexes.

Experimental

All chemicals were of the best commercial grade. Acetonitrile and dichloromethane were distilled from calcium hydride. Tetrabutylammonium perchlorate was recrystallized from ethyl acetate. Known complexes, *trans*-$RuCl_2(RNC)_4$ (**1**) (**1a**, R = 2,6-$Me_2C_6H_3$ (Xyl); **1b**, R = 2,4,6-$Me_3C_6H_2$ (Mes); **1c**, R = 4-Br-2,6-$Me_2C_6H_3$; **1d**, R = 2,4-$^tBu_2$-6-MeC_6H_2) and *ttt*-$RuCl_2(RNC)_2(PPh_3)_2$ (**2**) (**2a**, R = Xyl; **2b**, R = Mes) were prepared by the literature method [7]. *ttt*-$RuCl_2(RNC)_2(PPh_3)_2$ (**2c**, R = 4-Br-2,6-$Me_2C_6H_2$; **2d**, R = 2,4-$^tBu_2$-6-MeC_6H_2; **2e**, R = ^tBu; **2f**, R = 2,4,6-$^tBu_3C_6H_2$) and *ttt*-$RuCl_2(XylNC)_2[P(4\text{-}MeC_6H_5)_3]_2$ (**2g**) were prepared by an analogous procedure [7].

Thermal analyses were carried out on 2–10 mg samples under flowing nitrogen at a constant heating rate of 10 °C/min with a Rigaku Denki model TG-DSC (standard) instrument. DSC calibration was accomplished using α-Al_2O_3. Cyclic voltammograms were recorded using a HUSO 956B potentiostat and a HUSO 321 potential scanning unit. The electrochemical procedures were carried out according to literature methods [8]. The reference electrode is a $Ag/AgNO_3$–0.1 M [n-Bu_4N][ClO_4]/MeCN system. All potentials are versus a Cp_2Fe/Cp_2Fe^+ couple (1 Mm) in 0.1 M [n-Bu_4N][ClO_4]/MeCN solution (V versus $Ag/AgNO_3$). The products in the solid phase reactions were identified by comparison of their spectroscopic data with those of the complexes prepared separately in solution. IR spectra were measured as KBr disks on a Jasco A-100 spectrometer and electronic absorption spectra (UV–Vis) were recorded in CH_2Cl_2 with a Ubest-30 spectrometer. $^{31}P\{^1H\}$ NMR spectra were measured on a Jeol FX-100 spectrometer in $CDCl_3$ with external PPh_3 (in C_6D_6) as the reference.

The microanalyses of all complexes were in satisfactory agreement with the calculated values: C, ±0.42;

*Studies on the interaction of isocyanide with transition metal complexes. Part 39. For Part 38 see ref. 11.

**Author to whom correspondence should be addressed.

SSDI 0020-1693(93)03773-4

H, ±0.33; N, ±0.30. The IR and electronic spectra of the new complexes are listed as follows: *trans* and *ttt* isomers (IR: cm^{-1}; UV–Vis nm ($\epsilon \times 10^{-4}$ dm^3 mol^{-1} cm^{-1})): **2b** $^{31}P\{^1H\}$ NMR ($CDCl_3$): δ 37.44; **2c** (2092; 301.0 (4.60), 282.5 (5.10)); **2d** (2102; 308.5 (4.35), 279.0 (4.52)), $^{31}P\{^1H\}$ NMR ($CDCl_3$): δ 32.38; **2f** (2060; 266.0 (4.74)); **2g** (2100; 284.5 (7.38)); *cis* and *tcc* isomers (IR: cm^{-1}, UV–Vis nm ($\epsilon \times 10^{-4}$ dm^3 mol^{-1} cm^{-1})): **1a** (2162, 2112; ES, 269.0 (4.51)); **1b** (2148, 2104; 264.0 (8.8)); **1c** (2180, 2104; 273.0 (8.32)); **1d** (2170, 2102; 268.5 (6.62)); **2a** (2142, 2096; 273.0 (8.32)); **2b** (2150, 2110; 279.0 (5.48)), $^{31}P\{^1H\}$ NMR ($CDCl_3$): δ 28.22; **2c** (2146, 2096; 281.0 (7.40)); **2d** (2112, 2104; 282.5 (5.01)), $^{31}P\{^1H\}$ NMR ($CDCl_3$): δ 27.44; **2e** (2150, 2116; 325.0 (0.44), 265.5 (3.17)); **2f** (2118, 2068; 273.0 (4.59)); **2g** (2136, 2084; 279.0 (4.27)).

Results and discussion

Thermal isomerization

The solid-state isomerizations of *trans*-$RuCl_2(RNC)_4$ (**1**) and *ttt*-$RuX_2(RNC)_2(PR'_3)_2$ (**2**) are shown in Scheme 1.

The results of the thermal analyses are given in Table 1. Any endothermic or exothermic reaction observed by DSC below the temperature for which there is no mass-loss is likely due to a phase change or isomerization. Melting is an endothermic process, but isomerization is expected to be exothermic because the geometric transformation is from a less stable isomer to a thermodynamically more stable one. Figure 1 shows the DSC curve for complex **1a**. When **1a** was heated at 10 °C/min, three transitions (endothermic, exothermic and endothermic) were observed. The first endothermic process ($\Delta H = 4.2$ kJ/mol) began at about 92 °C. This corresponds to the melting point of the *trans* isomer. This is followed by an exotherm, beginning at about 171 °C. The exothermic process ($\Delta H_t = -21.0$ kJ/mol) is accompanied by a color change from yellow to pale yellow, the latter color corresponding to that of the *cis* isomer. That this process corresponds to the *trans*-to-*cis* isomerization of the complex was verified by cooling the sample after completion of the exothermic process and comparing the spectroscopic data with that of the *cis* isomer prepared separately in solution. The IR spectrum of the *trans* isomer showed only one N–C stretching frequency at 2135 cm^{-1}, but that of the product showed two bands at 2162 and 2112 cm^{-1}, suggesting the *cis* structure having C_{2v} symmetry. In the electronic spectrum of the *cis* isomer the three absorption bands at 265, 321 and 379(br) nm observed for the *trans* isomer disappeared and a new strong band was observed at 269 nm (Fig. 2). The third endothermic transition ($\Delta H = 6.6$ kcal/mol), beginning at about 229 °C corresponds to the melting point of the *cis* isomer. After these transitions were over, a mass-loss was observed, beginning at 252 °C. The DSC curve for complex **1b** showed successive endo- and exothermic reactions at *c.* 215 °C (Fig. 1(b)). The heat of the endothermic process was estimated as 9.2 kJ/mol and the heat of the exothermal one, as −0.4 kcal/mol. The formal process does not correspond to the complete melting of the *trans* isomer different from the thermal behavior of **1a**. When the *trans* isomer just begins to melt, an isomerization occurs simultaneously. This phenomena is verified by the fact that the heat of isomerization becomes smaller than that of **1a**, since it was compensated by the endothermic process of melting. No mass loss for complex **1b** was observed below 270 °C. The thermal behavior of **1d** is closely similar to that of **1b**; it proceeded with a successive melting and isomerization. For complex **1c**, melting was not observed, and the broad exotherm occurred in the range from *c.* 165 to 202 °C, being a solid-to-solid isomerization. The heat of isomerization ΔH_t was smaller than expected, and could not be estimated clearly because of the breadth of the peak.

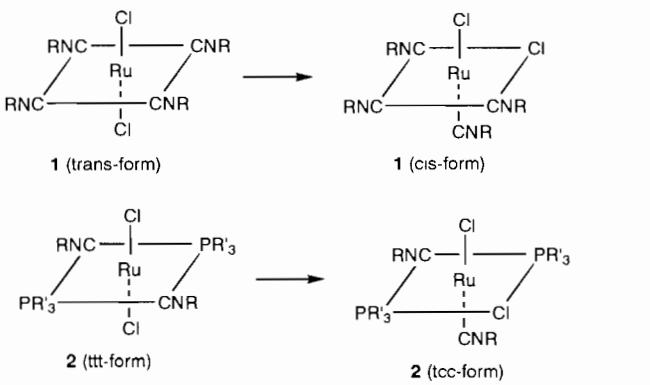

Scheme 1. Isomerizations of *trans*-$RuCl_2(RNC)_4$ and *ttt*-$RuCl_2(RNC)_2(PPh_3)_2$.

The DSC curve of **2a** showed an exotherm beginning at 204 °C, and then successive exothermic and endothermic processes, beginning at about 277 °C. The first transition corresponds to a *ttt–tcc* isomerization with a heat of isomerization of −28.1 kJ/mol. The isomerization was verified by the ^{31}P NMR spectrum of the sample. The $^{31}P\{^1H\}$ chemical shift of the *ttt* complex which appeared at δ 37.44 (from PPh_3 as an external reference) shifted to δ 28.22 for the *tcc* complex. The IR spectrum of *tcc*-**2a** showed two peaks for the terminal isocyanides, again suggesting C_{2v} symmetry for the complex. In the electronic spectrum a peak in the long wavelength region disappeared as was the case for **1a** (Fig. 3). The successive processes of the latter compound were accompanied by a mass-loss, corresponding to decomposition of the *tcc* isomer. A closely similar thermal process also occurred for **2b**. For complex **2d**,

TABLE 1. Results of differential scanning calorimetry and thermal gravimetric analysis for *trans*-$RuCl_2(RNC)_4$ and *ttt*-$RuCl_2(PPh_3)_2(RNC)_2$

	R[a]	Isomerization (ΔH_i)		Mass-loss (temperature)	
		Temp. (°C)	kcal/mol	Starting temp. (°C)	10% loss
1a[b]	Xyl	171–184	−21.0	−252	303
1b[c]	Mes	221–225	−1.7	−270	320
1c	4-Br-2,6-$Me_2C_6H_2$	165–202	−1.3	−245	316
1d[d]	2,4-$^tBu_2$-6-MeC_6H_2	268–275	−9.2	−283	300
2a[e]	Xyl	204–244	−28.1	−288	310
2b	Mes	222–262	−37.8	−322	344
2c	4-Br-2,6-$Me_2C_6H_2$	190–233	−27.3	−235	250
2d[f]	2,4-$^tBu_2$-6-MeC_6H_2	193–231	−28.1	−247	280
2e[g]	^tBu	184–231	−20.2	−231	250
2f[h]	2,4,6-$^tBu_3C_6H_2$			−200	230
2g[i]	Xyl	176–222	−47.5	−280	331

[a]Xyl = 2,6-$Me_2C_6H_4$; Mes = 2,4,6-$Me_3C_6H_2$ [b]Melting point of *trans* isomer (beginning at 92 °C, ΔH = 2.9 kcal/mol) and of *cis* isomer (beginning at *c.* 229 °C, ΔH = 6.6 kcal/mol). [c]Melting and isomerization occur simultaneously; melting (endotherm, 2.2 kcal/mol). [d]Successive endotherm (*c.* 260–268 °C, 4.5 kcal/mol for melting) and exotherm (268–275 °C, isomerization). [e]Successive exotherm (273–307 °C, ΔH = −3.3 kcal/mol) and endotherm (−307 °C, 12.7 kcal/mol) due to decomposition. [f]Endotherm (247–288 °C, 11.9 kcal/mol for melting). [g]Endotherm (231–277 °C, 46.7 kcal/mol for decomposition). [h]Endotherm (168–188 °C, 19.5 kcal/mol for melting). Isomerization did not occur. [i]$RuCl_2(XylNC)_2[P(o\text{-tolyl})_3]_2$.

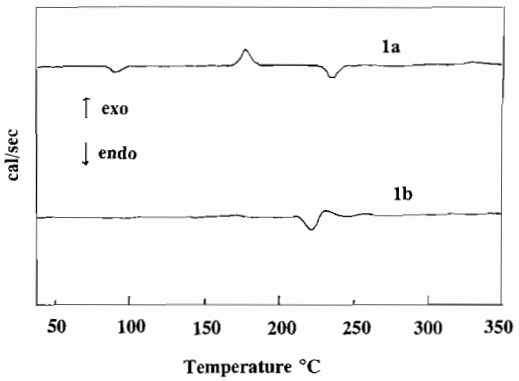

Fig. 1. DSC curves of *trans*-$RuCl_2(XylNC)_4$ (*trans*-**1a**) (a) and *trans*-$RuCl_2(MesNC)_4$ (*trans*-**1b**) (b). Heating rate: 10 °C/min.

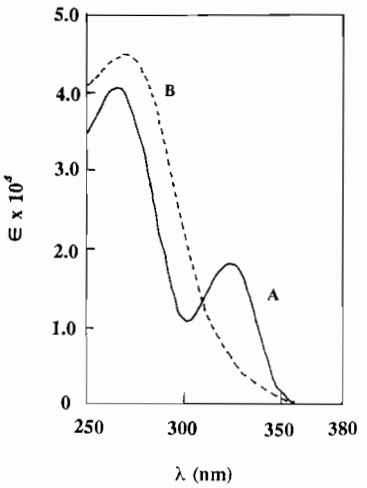

Fig. 2. Electronic absorption spectra in CH_2Cl_2 of *trans*-$RuCl_2(XylNC)_4$ (*trans*-**1a**) (A) and *cis*-$RuCl_2(XylNC)_4$ (*cis*-**1a**) (B).

the exothermic reaction began at *c.* 200 °C, due to the isomerization of the *ttt* isomer to the *tcc* one, and the endothermic process of 50.0 kJ/mol appeared at *c.* 247 °C. Since the latter process was accompanied by a mass-loss, it corresponds to the decomposition of the complex. Complex **2f** having sterically bulky isocyanides, *ttt*-$RuCl_2(2,4,6\text{-}^tBu_3C_6H_2NC)_2(PPh_3)_2$, showed an endothermic reaction (81.9 kJ/mol) beginning at about 165 °C, due to the melting of the *ttt* isomer and there was no exotherm. Further an isomerization was not observed visually or spectroscopically, probably because of steric bulk of the isocyanide ligands. The mass-loss began at about 195 °C. The DSC curve of complex **2e** showed two successive thermal processes (exotherm and endotherm); the former began at 184 °C, corresponding to the heat of isomerization (−20.2 kJ/mol) and the latter gained the energy of 208.7 kJ/mol, accompanied by a mass-loss of *c.* 35%. This mass-loss corresponds to the total weight of isocyanide and triphenylphosphine, but the products of this decomposition are not known.

Complexes **2c** and **2g** isomerized from the *ttt* to the *tcc* form without melting, proceeding through the solid-to-solid rearrangement.

The heats of isomerization of **1**, ΔH_i, obtained from the DSC curve are −9.2 to −5.0 kJ/mol and those of **2**, −20.2 to −47.5 kJ/mol, suggesting that ruthenium isocyanide complexes isomerize more easily than phosphine complexes. These ΔH_i values are similar to those of the solid-state isomerization of *trans*-$RuCl_2(CO)_2(PR_3)_3$ and *ttt*-$RuCl_2(CO)_2(PR_3)_2$ [4] but

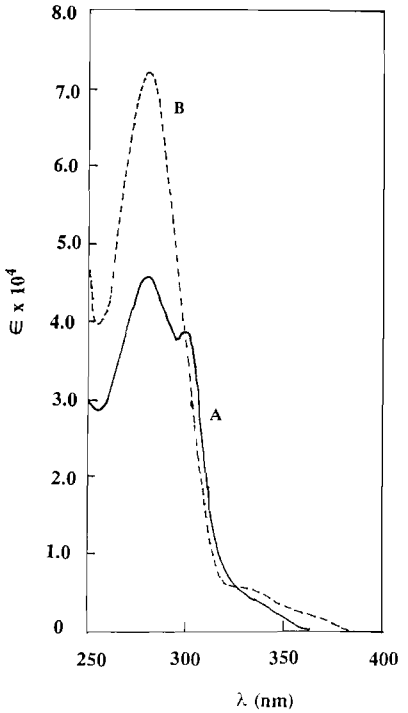

Fig. 3. Electronic absorption spectra in CH_2Cl_2 of *ttt*-$RuCl_2(MesNC)_2(PPh_3)_2$ (*ttt*-**2b**) (A) and *tcc*-$RuCl_2(MesNC)_2(PPh_3)_2$ (*tcc*-**2b**) (B).

are larger than those of the square planar $PtCl_2(L)_2$ (L = PEt_3, PPr_3, $AsEt_3$, $SbEt_3$) complexes (4.2–10.5 kJ/mol) [9]. The differences in the isomerization energies may result from differences in the coordination numbers. The thermal stabilities of the ruthenium complexes are relatively high and dependent on the structures of complexes.

Electrochemistry

The electrochemical data for oxidation of *trans*- and *cis*-$RuCl_2(RNC)_4$ (*trans*-**1** and *cis*-**1**), *ttt*-$RuCl_2(RNC)_2(PPh_3)_2$ and *tcc*-$RuCl_2(RNC)_2(PR'_3)_2$ complexes (*ttt*-**2** and *tcc*-**2**) are given in Table 2.

Previously we have reported that electrochemical oxidations of **1a** and **2a** proceed through a quasi-reversible one-electron transfer [7]. Thus, redox cycles of *cis*-**1** and *tcc*-**2** are quasi-reversible ($i_{pa}/i_{pc} \alpha 1.0$) and correspond to a one-electron redox reaction as judged by comparison with ferrocene as an internal calibrant. Oxidation potentials were a function of stereochemistry and ligands. The oxidation potentials of *cis*-**1** and *tcc*-**2** are larger than those of the corresponding *trans*-**1** and *ttt*-**2**, respectively, showing that the latter complexes are oxidized more readily than the former ones. They increased in the order 2,4-^{t}Bu$_2$-6-MeC_6H_2NC < MesNC < XylNC for **1**, and MesNC < 2,4-^{t}Bu$_2$-6-MeC_6H_2NC < XylNC for **2**. The tris(*p*-tolyl)-phosphine complex **2g** is oxidized more readily than the triphenylphosphine complex **2a**. These trends are in agreement with the fact that an increase in the electron density on the metal leads to an easier oxidation.

TABLE 2. Electrochemical data for the oxidations[a] of $RuCl_2(RNC)_4$ (**1**) and $RuCl_2(RNC)_2(PPh_3)_2$ (**2**)

	R	Form	$i_{pc/pa}$	$E_{1/2}$[b]	ΔE[c] (V)
1a	2,6-$Me_2C_6H_3$	*trans*	1.02	0.76	0.10
		cis	1.02	1.33	0.10
1b	2,4,6-$Me_3C_6H_2$	*trans*	1.03	0.70	0.08
		cis	1.14	1.06	0.08
1d	2,4-^{t}Bu$_2$-6-MeC_6H_2	*trans*	1.07	0.67	0.13
		cis[d]			
2a	2,6-$Me_2C_6H_3$	*ttt*	1.07	0.38	0.08
		tcc	1.09	0.87	0.09
2b	2,4,6-$Me_3C_6H_2$	*ttt*	1.05	0.36	0.08
		tcc	1.21	0.83	0 08
2c	2,4-^{t}Bu$_2$-6-MeC_6H_2	*ttt*	1.08	0.32	0.08
		tcc	1.25	0.87	0.06
2g[e]	2,4-$Me_2C_6H_3$	*ttt*	1.06	0.72	0.08
		tcc	1.30	0.80	0.08

[a]Measured in a 0.1 M solution of [^{n}Bu$_4$N][ClO_4]/CH_2Cl_2 at a Pt button electrode (1.6 mm ϕ); reference electrode: Ag/$AgNO_3$ in a 1 mM [^{n}Bu$_4$N][ClO_4]/CH_3CN solution; potentials vs. Cp_2Fe/Cp_2Fe^+ couple. Sample concentration: *c.* 0.1 mM; scan rate: 0.2 V/s. [b]$E_{1/2} = (|E_{pa}| + |E_{pc}|)/2$. [c]$\Delta E = ||E_{pa}| - |E_{pc}||$. [d]Not measured because of low solubility. [e]$RuCl_2(RNC)_2[P(4\text{-}MeC_6H_5)_3]_2$.

TABLE 3. The HOMO and total energies of $RuCl_2(HNC)_4$ and $RuCl_2(PH_3)_2(HNC)_2$

Compound	Form	HOMO (eV)	Total energy (eV)
$RuCl_2(HNC)_4$	*trans*	−9.76	−1056.23
	cis	−9.85	−1056.53
$RuCl_2(PH_3)_2(HNC)_2$	*ttt*	−9.41	−941.99
	tcc	−9.66	−942.26

Conclusions

In an attempt to gain some information on the *trans*-to-*cis* and *ttt*-to-*tcc* isomerizations and on the difference in the redox potentials as a function of the stereochemistry of the complexes, EHMO calculations of each configuration of the idealized $RuCl_2(HNC)_4$ and $RuCl_2(HNC)_2(PH_3)_2$ complexes were performed [10]. The calculated results of the HOMO and total energies are given in Table 3.

In the oxidation reactions the electron removed comes out of the highest occupied molecular orbital (HOMO). Thus, the oxidation potential should show a relation with the HOMO energy. The HOMO energies of *trans*-

1 and *ttt*-**2** are higher by *c.* 8 to 25 kJ/mol (0.09 to 0.25 eV) than those of the corresponding *cis*-**1** and *tcc*-**2**, respectively, being in close agreement with the fact that the former complexes are more easily oxidized than the latter. On the basis of the total energies, *cis*-$RuCl_2(RNC)_4$ and *tcc*-$RuX_2(PR_3)(R'NC)_2$ are thermodynamically more stable than the corresponding *trans* and *ttt* isomers. The total energy difference between *cis*- and *trans*-$RuCl_2(HNC)_4$ is 29.0 kJ/mol (0.3 eV) which is larger than that of $RuCl_2(HNC)_2(PH_3)_2$ (26.0 kcal/mol (0.27 eV)) (Table 3). These results suggest that the *trans–cis* isomerization proceeded with thermodynamic control. Contrary to the calculations, the larger heats of isomerization measured for phosphine complexes than for isocyanide complexes are likely a result of the steric bulk of the phosphine ligands.

Acknowledgements

We thank Professor S. Takahashi and Dr K. Onitsuka of Osaka University for measurements of the ^{31}P NMR spectra.

References

1 M. Fushimi, M. Suzuki and A. Uehara, *Bull. Chem. Soc. Jpn., 61* (1988) 1809.
2 R. Ellis, T.A. Weil and M. Orchin, *J Am. Chem. Soc, 92* (1970) 1078.
3 (a) Y.N. Kukushkin, V.F. Budanova, G.N. Sedova and V.G. Pogareva, *Zh. Neorg. Khim., 22* (1977) 1305; (b) G.N. Sedova and L.N. Demchenko, *Neorg. Khim., 26* (1981) 435, and refs. therein.
4 D.W. Krassowski, K Reimer, H.E. LeMay, Jr. and J.H. Nelson, *Inorg. Chem., 27* (1988) 4307.
5 B.E. Prater, *J. Organomet. Chem., 34* (1972) 379.
6 T. Tsuihiji, T. Takiyama and A. Sugimori, *Bull. Chem. Soc. Jpn., 52* (1979) 3451.
7 Y. Yamamoto, T. Tanase, T. Date, Y. Koide and K. Kobayashi, *J Organomet Chem., 386* (1990) 365.
8 Y. Yamamoto, K. Takahashi, K. Matsuda and H. Yamazaki, *J Chem Soc, Dalton Trans.,* (1987) 1833.
9 J. Chatt and R.G. Wilkins, *J. Chem. Soc.,* (1952) 273; (1952) 4300; (1953) 70, 1956.
10 H. Kobayashi, EHMO program, 1988.
11 Y. Yamamoto and H. Yamazaki, *Inorg. Chim. Acta,* to be published.

Appendix

All calculations were carried out on a personal computer PC-9801VX with the EHMO program (by Kobayashi in Kyoto Prefecture University). The parameters used in the EHMO calculations are involved in the program [10]. The Ru–C, C–N, N–H, Ru–P, P–H and Ru–Cl distances were set to 2.03, 1.17, 1.01, 2.41, 1.42 and 2.30 Å, respectively. The structures of the complexes were idealized to be octahedral. The Ru–C–N and C–N–H bond angles were idealized to be linear, and the P atoms were given idealized sp^3 hybridization.